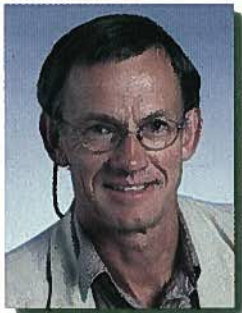# Direct Displacement-Based Design of Precast/Prestressed Concrete Buildings

**M. J. Nigel Priestley, Ph.D.**
Emeritus Professor
Department of Structural Engineering
University of California at San Diego
La Jolla, California
and
Co-Director
European School for Advanced
Studies in Reduction of Seismic Risk
Pavia, Italy

*The five-story PRESSS precast/prestressed concrete building tested at the University of California at San Diego was designed in accordance with a new seismic design procedure known as Direct Displacement-Based Design (DDBD). This procedure enables precast/prestressed concrete buildings (and other structures) to be designed to respond in the design-level earthquake to specified displacement limits, corresponding to acceptable damage limit states, while taking into account the special ductility and damping characteristics of the structural system. This paper outlines the fundamentals of this procedure as related to precast concrete buildings. A numerical design example is included to show the application of the DDBD method.*

Precast concrete structures are conveniently divided into two main categories: those which emulate monolithic reinforced concrete structures (reinforced concrete emulation), and those with ductility concentrated at the connections (jointed systems).

In reinforced concrete emulation systems, ductility may still occur at the connections between precast elements, but will be spread over a plastic hinge length similar to that in a monolithic reinforced concrete structure, by bond between concrete and reinforcing steel. In jointed systems, typically one major crack occurs at the connection, and the precast elements remain elastic.

Generally, reinforced concrete emulation systems rely on bonded mild steel reinforcement for strength and ductility. Jointed systems for seismic response generally incorporate unbonded prestressing steel, with or without additional mild steel reinforcement to provide structural resilience. In recent years, research in the United States, through the PRESSS (Precast Seismic Structural Systems) research program, has concentrated on developing efficient jointed systems.[1]

As a consequence of the differences in structural concepts, the two categories display different hysteretic force-deformation characteristics. Reinforced concrete emulation systems typically have comparatively high hysteretic damping, and moderate ductility capacity, and may display significant residual displacement after response to a major earthquake.

On the other hand, jointed systems employing unbonded prestressing steel typically absorb less energy, and hence have less hysteretic damping, but have higher ductility capacity, insofar as it is appropriate to discuss ductility in systems which do not have a well-defined yield displacement. Jointed systems with unbonded prestressing also exhibit low or zero residual displacement at design levels of seismic response.

These different characteristics are illustrated in Fig. 1, which also includes the elasto-plastic hysteresis loop shape for comparison. In Fig. 1, which illustrates the response for two complete cycles to the same peak displacement, the residual displacement is indicated as $d_{EP}$, $d_{RC}$, and $d_J$, for elasto-plastic, reinforced concrete, and jointed systems, respectively.

It is clear that some recognition of the differences in structural response between the two categories needs to be made in the design process. In fact, this is essential, as current design requirements in the United States severely penalize precast concrete by requiring the precast structural system to be demonstrably equivalent to reinforced concrete.

This approach generally requires expensive and time-consuming testing, and the equivalence cannot be satisfied by many of the jointed systems that have been developed in the PRESSS program. Some progress towards accommodating reinforced concrete emulation precast structures in a force-based seismic design environment is being achieved by current activities of the American Concrete Institute.[2,3]

On the other hand, the excellent performance of recent PRESSS tests, and in particular the five-story precast superassemblage tested at UCSD and reported recently in the PCI JOURNAL,[4]



(a) Reinforced concrete

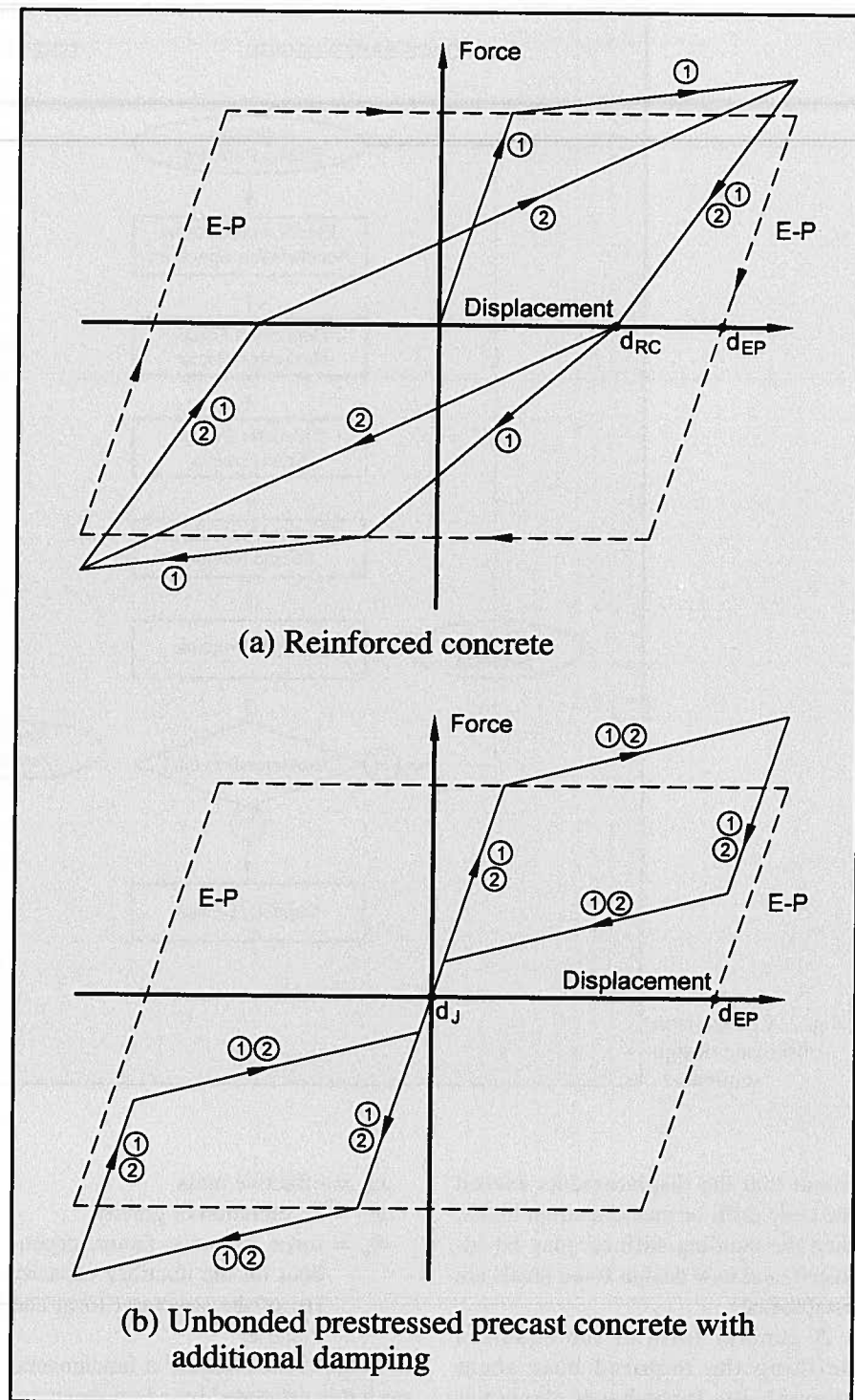(b) Unbonded prestressed precast concrete with additional damping

Fig. 1. Comparison of elasto-plastic and realistic hysteretic response.

indicates that means for routine design and acceptance of the jointed PRESSS concepts must be established as a matter of urgency.

Current seismic design in the United States, and in most of the world, is carried out in accordance with force-based design principles. In force-based design, elastic forces are based on initial elastic estimates of building period together with a design acceleration spectrum for 5 percent damping. Design force levels are reduced from the elastic level by dividing by a code-specified force-reduction factor, reflecting assumed ductility capacity.

Displacements are checked at the end of the design process, based on assumed relationships between elastic and inelastic displacements. If it is

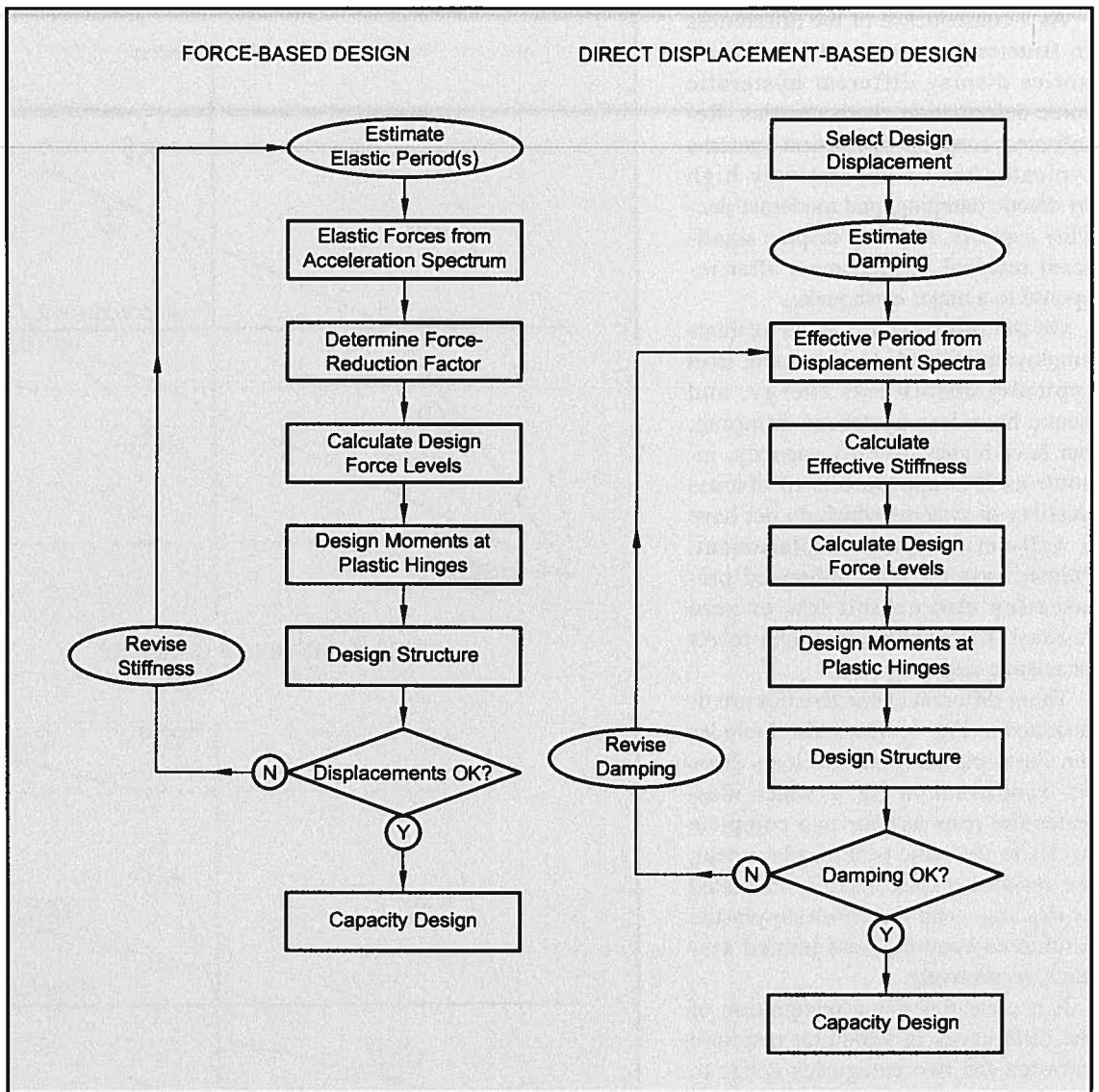FORCE-BASED DESIGN       DIRECT DISPLACEMENT-BASED DESIGN

Fig. 2. Comparison of seismic design sequences.

found that the displacements exceed the code drift, or material strain limits, then the building stiffness may be adjusted, and new design force levels are established.

A general form of the equation defining the required base shear strength for force-based design is given by Eq. (1):

$$V_B = \frac{C_T I (g m_e)}{R_\mu} \qquad (1)$$

where

$C_T$ = basic seismic coefficient dependent on seismic intensity, soil condition and period, $T$

$I$ = an importance factor reflecting different levels of acceptable risk for different building functions

$m_e$ = effective mass

$g$ = acceleration of gravity

$R_\mu$ = force reduction factor, dependent on the ductility capacity ($\mu$) of the structural form and material

In the United States,[5] a fundamental period is estimated based on structural form, material, and building height, rather than on geometry and member stiffness. The period equation is of the form:

$$T = C_1 (h_n)^{0.75} \qquad (2)$$

where $h_n$ is the building height and $C_1$ is a coefficient dependent on the structural system.

Although modal analysis based on realistic member stiffness is permitted, the base shear so calculated must not

be less than that calculated from Eq. (2), using an equivalent lateral force analysis, by more than 20 percent.

Eq. (2) generally results in much shorter periods, and hence higher elastic seismic design forces, than would result from structural analysis using realistic member stiffnesses. To some extent, this is compensated by the specification of unrealistically high force reduction factors, $R_\mu$.

Although current seismic design practice in the United States generally results in acceptable levels of seismic design force for reinforced concrete structures, it is unsuitable for the design of jointed precast systems, as noted above. It is difficult to define appropriate force reduction factors for jointed systems, since yield displacement, and hence ductility capacity,
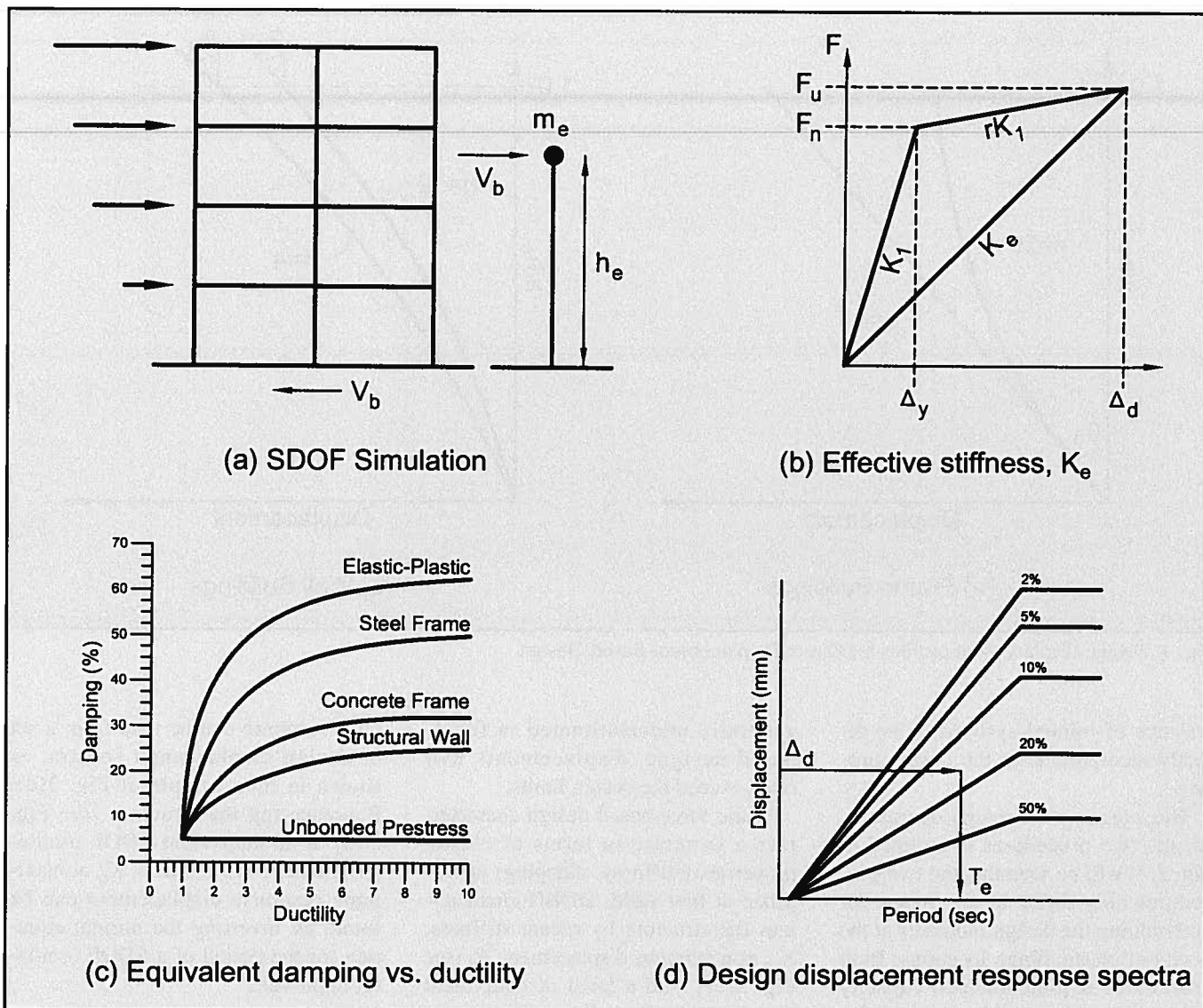
Fig. 3. Displacement-based design fundamentals.

cannot be readily defined.

Further, force-reduction factors seem inappropriate for jointed precast systems, since design displacements will almost always be limited by code-specified drift limitations intended to limit non-structural damage. Hence, force-reduction factors, which are intended to limit structural damage, will not govern the design. Hysteretic energy absorption may be considerably less than for reinforced concrete structures, creating a tendency for precast structures to develop larger displacements for a given elastic stiffness and strength than would be the case for reinforced concrete structures.

In recent years, considerable research effort has been put into the development of displacement-based, or performance-based, seismic design.[6,7]

This is in recognition that it is displacements (or material strains, which can readily be converted to displacements) that are better indicators of damage potential than are forces. In fact, it can be shown that damage potential is rather poorly correlated with strength.

One of the more developed methods, Direct Displacement-Based Design (DDBD), has been specifically developed with precast concrete in mind, and was used to design the PRESSS five-story precast prestressed concrete test building.[4] This paper discusses the theoretical basis for DDBD, and outlines the sequence of design steps. As will be seen, the procedure is extremely simple and rational, but requires a reorganization of the way seismic design is perceived.

## DIRECT DISPLACEMENT-BASED DESIGN (DDBD)

In DDBD, the design drift is the starting point, where drift is defined as the inter-story displacement divided by the story height. The structure is characterized by secant stiffness and damping at maximum displacement response, and the design forces necessary to achieve the design drift limit are directly found.

The assumed level of damping is checked, and if necessary, the design forces are adjusted, though the adjustments are generally small, and frequently unnecessary. Unlike force-based design, the use of damping values characteristic of the hysteretic force-displacement response enables the special force-displacement charac-
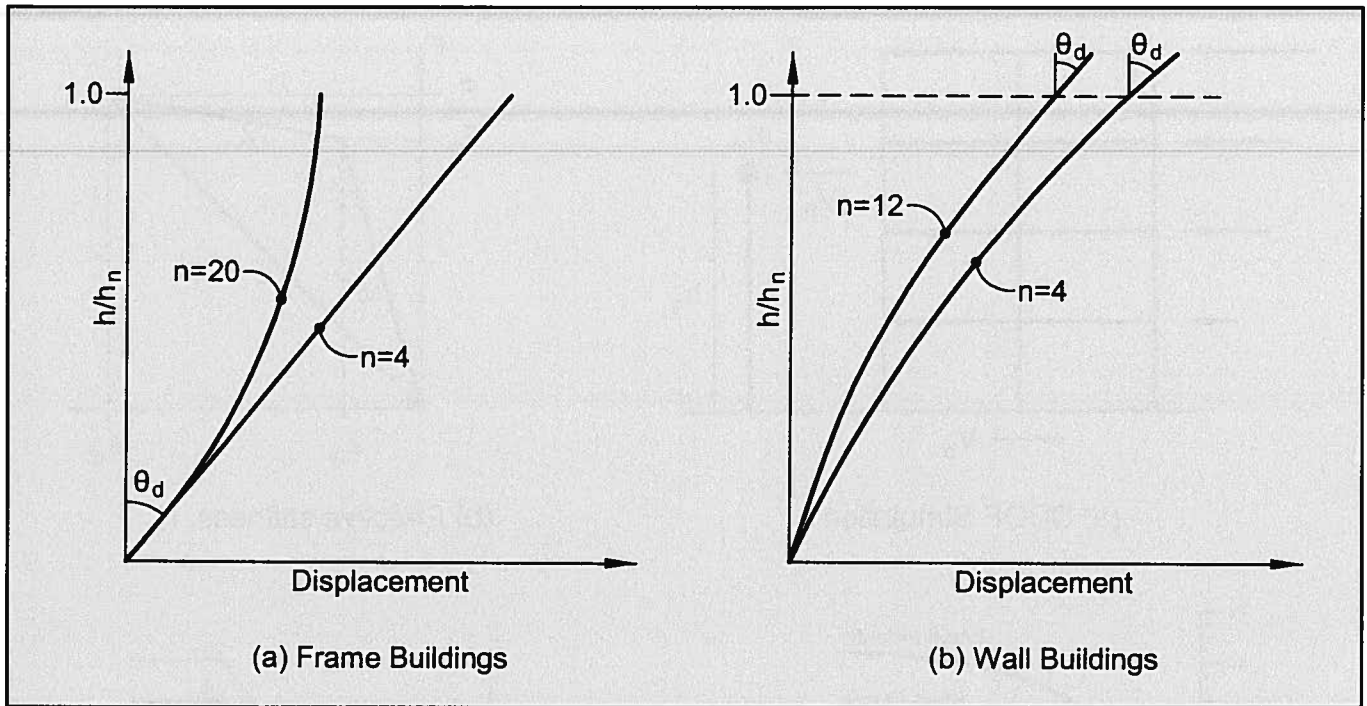
Fig. 4. Design displacement profiles for Direct Displacement-Based Design.

teristics of jointed systems to be directly incorporated in the design process.

The sequence of design operations for the two procedures is outlined in Fig. 2. It will be seen that the two procedures only differ in the means for determining the design moments at the potential plastic hinge locations. Both procedures require standard capacity protection measures[8] to ensure that plastic hinges develop only at intended locations, and that non-ductile inelastic modes of deformation, such as shear failure, are inhibited.

The design procedure is described in detail in the following. The design approach attempts to produce a structure which would achieve, rather than be bounded by, a given performance limit state under a given seismic intensity, essentially resulting in uniform-risk structures, which is philosophically compatible with the uniform-risk seismic spectra incorporated in most codes.

Note that force-based design provides upper bounds for displacement which, in theory, will only be achieved by a small fraction of designed structures. The risk of damage under the design level earthquake will thus vary from structure to structure. In fact, since member stiffnesses are

generally underestimated in force-based designs, displacements will often exceed the design limits.

While force-based design characterizes a structure in terms of elastic properties (stiffness, damping) appropriate at first yield, DDBD characterizes the structure by secant stiffness, $K_e$, at maximum displacement $\Delta_d$ [see Fig. 3(b)], and a level of equivalent viscous damping appropriate to the hysteretic energy absorbed during inelastic response. Thus, as shown in Fig. 3(c), for a given level of ductility demand, a precast concrete building connected with unbonded prestressing tendons will be assigned a lower level of equivalent viscous damping than a reinforced concrete structural frame building designed for the same level of ductility demand, as a consequence of "thinner" hysteresis loops. The approach used to characterize the structure using a SDOF representation, with secant stiffness to maximum displacement response and equivalent damping is based on the "substitute structure" analysis procedure developed by Shibata and Sozen.[9]

With the design displacement $\Delta_d$ determined, as discussed subsequently, and the damping estimated from the expected ductility demand, the effective period, $T_e$, at maximum displace-

ment response can be read from a set of design displacement spectra, as shown in the example of Fig. 3(d). Representing the structure [see Fig. 3(a)] as an equivalent SDOF oscillator, the effective stiffness, $K_e$, at maximum response displacement can be found by inverting the normal equation for the period of a SDOF oscillator to provide:

$$K_e = 4\pi^2 m_e / T_e^2 \qquad (3)$$

where $m_e$ is the effective mass, defined subsequently.

From Fig. 3(b), the design base shear at maximum response is thus:

$$V_B = K_e \Delta_d \qquad (4)$$

The design concept is, therefore, very simple, and such complexity as exists relates to determination of the "substitute structure" characteristics, determination of the design displacement, and development of design displacement spectra.

**Design Displacement** — The design displacement for the equivalent SDOF model of a multistory building is given by:

$$\Delta_d = \sum_{i=1}^{n} \left( m_i \Delta_i^2 \right) / \sum_{i=1}^{n} \left( m_i \Delta_i \right) \qquad (5)$$

where $m_i$ and $\Delta_d$ are the story masses and displacements, respectively, at the design response level.

This assumes that the inelastic first-mode shape rather than the elastic mode shape should be used to determine the generalized displacement coordinate of the SDOF model. This is consistent with characterizing the structure by its secant stiffness to maximum response. In fact, the inelastic and elastic first-mode shapes are generally very similar.[10]

Eq. (5) requires knowledge of the design displacement profile up the height of the building, which can be defined by a critical drift, and a characteristic displacement shape. In most cases for precast buildings, the critical drift will be dictated by code drift limits, as previously discussed.

In general, however, the peak drift can be expressed as:

$$\theta_d = \theta_y + \theta_p \le \theta_c \qquad (6)$$

where the design drift $\theta_d$ is comprised of elastic ($\theta_y$) and plastic ($\theta_p$) components and must not exceed the code limit $\theta_c$.

Typical values for $\theta_c$ are within the range of 2 to 2.5 percent. The critical location for $\theta_d$ is likely to be at the lower floors of a frame building. For wall buildings, the drift based on strain limitations will be critical at the wall base, but for non-structural elements, the higher drift at the roof level will be critical.

Walls with unbonded prestressing will rarely be governed by material strain limitations, and hence it is the drift at the top floors that will be critical. More research is needed, however, to investigate the influence of a higher mode response on drifts in the upper stories of frame buildings.

The yield drift depends on structural geometry and material sizes. Extensive analyses of structural members for conventional or reinforced concrete emulation systems[11,12] have established that the yield drift and displacement can be estimated from the following member dimensionless yield curvatures. These values have been found to be relatively insensitive to the axial load ratio and reinforcement ratio within the normal range of these variables adopted for reinforced concrete design:

Beams (rectangular or flanged):
$$h_b \phi_y = 1.7 \varepsilon_y \quad (+/-) \ 10 \ \text{percent} \quad (7a)$$

Circular columns:
$$D \phi_y = 2.35 \varepsilon_y \quad (+/-) \ 15 \ \text{percent} \quad (7b)$$

Rectangular columns:
$$h_c \phi_y = 2.12 \varepsilon_y \quad (+/-) \ 10 \ \text{percent} \quad (7c)$$

Rectangular walls:
$$l_w \phi_y = 2.0 \varepsilon_y \quad (+/-) \ 10 \ \text{percent} \quad (7d)$$

where $h_b$, $D$, $h_c$ and $l_w$ are the depth, or diameter, of beams, circular columns, rectangular columns, and walls, respectively, and $\varepsilon_y$ is the yield strain of the flexural reinforcement.

Note that the form of the components of Eq. (7) indicates that the yield curvature is independent of strength, and hence strength and stiffness are directly proportional. This points to a fundamental error in current force-based design, where strength is allocated between members in proportion to their stiffness.

For reinforced concrete frame structures, "yield" drifts may be estimated[12] by:

$$\theta_y = 0.5 \varepsilon_y \frac{l_b}{h_b} \qquad (8)$$

where $l_b$ is the bay length (distance between adjacent column centerlines) and $h_b$ is the beam depth.

Note that Eq. (8) was developed from Eq. (7a), making average allowances for column and joint flexibility, and for member shear deformations. The predictions of Eq. (8) were compared with results from 43 beam-column test assemblages with different material strengths, proportions and column axial load levels, and was found to provide a good estimate of the experimental yield drifts, with surprisingly little scatter.[12] Typical yield drifts from Eq. (8) are in the range of 0.006 to 0.012; much larger than is generally assumed for reinforced concrete.

Note that the yield drift given by Eq. (8) refers to the "corner" of the equivalent bilinear force-displacement response, and thus generally exceeds the true first-yield condition. This definition was adopted because it is directly compatible with assumptions made analytically in relating force reduction factors to displacement ductility factors.

When the frames have beams with unbonded prestressing, the elastic stiffness will be much higher than implied by Eqs. (7) and (8), and the yield drift can be estimated, with sufficient accuracy for ductility calculations, by:

$$\theta_y = 0.0004 \frac{l_b}{h_b} \qquad (9)$$

Eq. (9) assumes that the effective yield displacement of a prestressed frame is approximately 40 percent of that of a reinforced concrete frame with identical member sizes, reinforced with Grade 60 ($f_y = 414$ MPa) reinforcement.

Having determined the critical drift, the design displacements, $\Delta_i$, at different stories ($i$) can be estimated from characteristic displacement profiles at maximum response based on inelastic time history analysis. The following equations, though approximate, have:

For building frames:
With $n < 4$
$$\Delta_i = \theta_d h_i \qquad (10a)$$

With $4 < n < 20$
$$\Delta_i = \theta_d h_i \left[ 1 - \frac{0.5 h_i (n - 4)}{16 h_n} \right] \quad (10b)$$

With $n > 20$
$$\Delta_i = \theta_d h_i \left( 1 - 0.5 h_i / h_n \right) \quad (10c)$$

where $n$ is the number of stories, and $h_i$ and $h_n$ are the heights to the $i$th story and roof, respectively.

Note that Eq. (10) implies a displacement profile that changes from linear for low-rise frames to parabolic for frames of twenty stories or more (see Fig. 4a).

For reinforced concrete cantilever wall buildings, the maximum drift occurs at the top of the building (see Fig. 4b). From Eq. (7d), assuming a linear distribution of curvature with height, the elastic yield drift at roof level is:
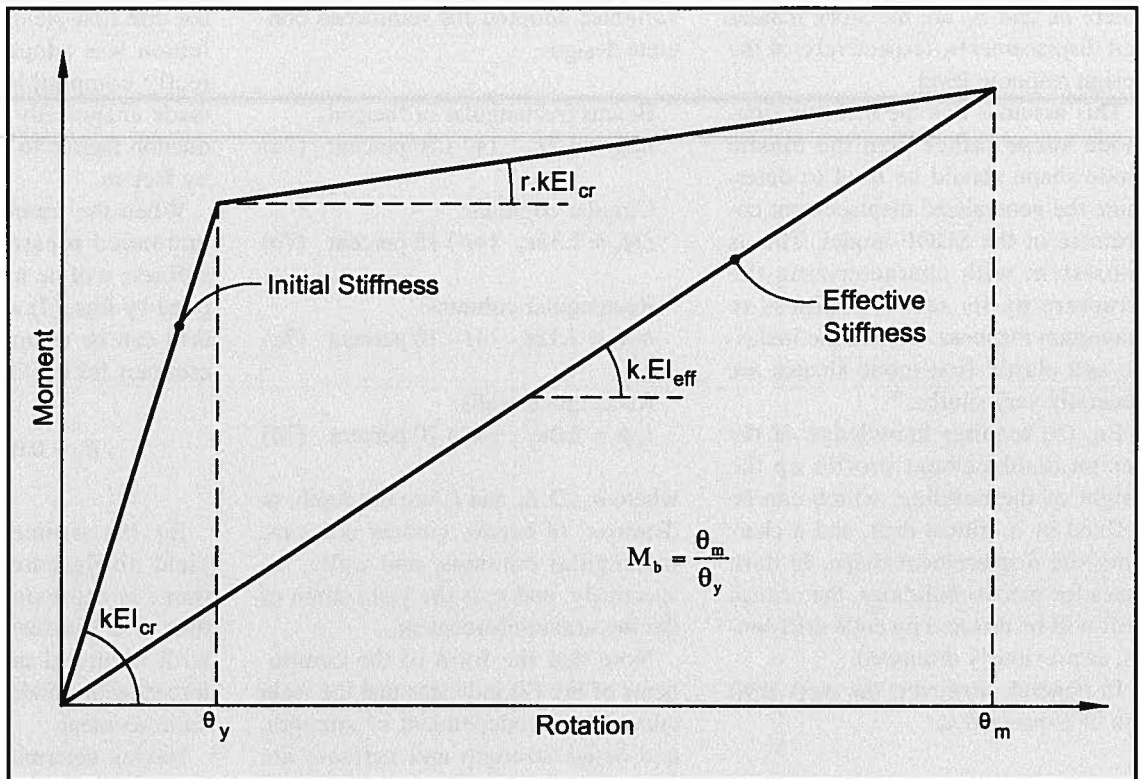
$$M_b = \frac{\theta_m}{\theta_y}$$

Fig. 5. Typical beam moment-rotation response.

$$\theta_y = \varepsilon_y h_n / l_w \qquad (11)$$

Hence, Eq. (6) becomes:

$$\theta_d = \varepsilon_y h_n / l_w + (\phi_m - \phi_y)l_p \le \theta_c \qquad (12)$$

where $l_p$ is the plastic hinge length and $\phi_y$ and $\phi_m$ are yield and maximum curvatures, respectively.

The design displacement profile for the wall can then be estimated[14] as:

$$\Delta_i =$$

$$0.67\varepsilon_y \frac{h_i^2}{l_w}\left[1.5 - \frac{h_i}{2h_n}\right] +$$

$$\left[\theta_d - \frac{\varepsilon_y h_n}{l_w}\right]\left[h_i - \frac{l_p}{2}\right] \qquad (13a)$$

For cantilever wall buildings where the wall strength is primarily provided by unbonded prestressing, the deformation at maximum displacement response will be dominated by base rotation due to wall rocking, resulting in an almost linear displacement profile. Thus, for walls up to ten stories high, the displacement profile of Eq. (13a) can be simplified to:

$$\Delta_i = \Delta_d h_i \qquad (13b)$$

**Effective Mass** — From consideration of the mass participating in the first inelastic mode, the effective system mass for the equivalent SDOF system is:

$$m_e = \sum_{i=1}^{n}\left(m_i\Delta_i\right)/\Delta_d \qquad (14)$$

Typically, for building structures:

$$m_e \approx 0.8\sum m_i \qquad (15)$$

**Effective Damping** — The effective damping depends on the structural system and the displacement ductility factor $\mu = \Delta_d/\Delta_y$, where the design and yield displacement may be calculated as above.

The following approximate relationships, based on the shape of the modified Takeda hysteresis rule[15] may be used to relate damping ($\xi$), expressed as a percentage of critical damping to ductility factor for different structural systems:

Reinforced concrete frames:
$$\xi = 5 + 30(1 - \mu^{-0.5}) \text{ percent} \qquad (16a)$$

Reinforced wall structures:

$$\xi = 5 + 23(1 - \mu^{-0.5}) \text{ percent} \qquad (16b)$$

Frames or walls with unbonded prestressing:
$$\xi = 5 \text{ percent} \qquad (16c)$$

For hybrid frames or walls where the strength and energy dissipation are provided by a combination of unbonded prestressing steel and mild steel reinforcement, the effective damping should be interpolated between Eqs. (16c) and (16a) in proportion to the fraction of flexural strength provided by the mild steel reinforcement.

**Design Displacement Spectra** — A major difference from force-based design is that DDBD utilizes a set of displacement-period spectra [see Fig. 3(d)] for different levels of equivalent viscous damping, rather than the acceleration-period spectra for 5 percent damping adopted by most force-based codes. It is appropriate to limit code peak spectral response displacements, since at long periods, structural displacements tend to decrease, eventually equaling the peak ground displacement.

The European Seismic Code EC8[16] adopts a critical period of $T = 3$ sec-

onds above which displacements are considered to be independent of period and equal to the $T = 3$ seconds value. Geotechnical considerations indicate that the cap period should depend on the foundation condition, with lower periods applying for rock than for soft soil. For alluvial soils, a cap period of 4 seconds appears to be appropriately conservative.

Displacement spectra should be directly developed for displacement-based design. However, acceptable spectra may be developed from the design acceleration spectrum for 5 percent damping as follows:

$$\Delta_{(T,5)} = S_{(T,5)} g T^2 / (4\pi^2) \qquad (17)$$

$$\Delta_{(T,\xi)} = \Delta_{(T,5)} \left[ \frac{7}{2 + \xi} \right]^{1/2} \qquad (18)$$

where $S_{(T,5)}$ is the 5 percent spectral response acceleration at period $T$ expressed as a fraction of the acceleration due to gravity, $g$, and $\Delta_{(T,5)}$ and $\Delta_{(T,\xi)}$ are the spectral displacements at period $T$ for 5 percent and $\xi$ percent damping, respectively.

Eq. (18) is taken from EC8.[16] Similar equations, differing only slightly from Eq. (18), have been developed by others (e.g., see Reference 17).

## Distribution of Base Shear Force

The base shear calculated in accordance with the above procedure should be vertically distributed based on the vertical mass and displacement profiles. Thus:

$$F_i = V_B(m_i \Delta_i) / \sum_{i=1}^{n} (m_i \Delta_i) \qquad (19)$$

Similarity with force-based design will immediately be apparent. The difference is that the design displacement profile, rather than a height-proportional displacement (which in effect assumes a linear distribution of elastic displacements with height), is adopted.

## Analysis for Member Design Actions

Since Direct Displacement Based Design considers the structural condi-
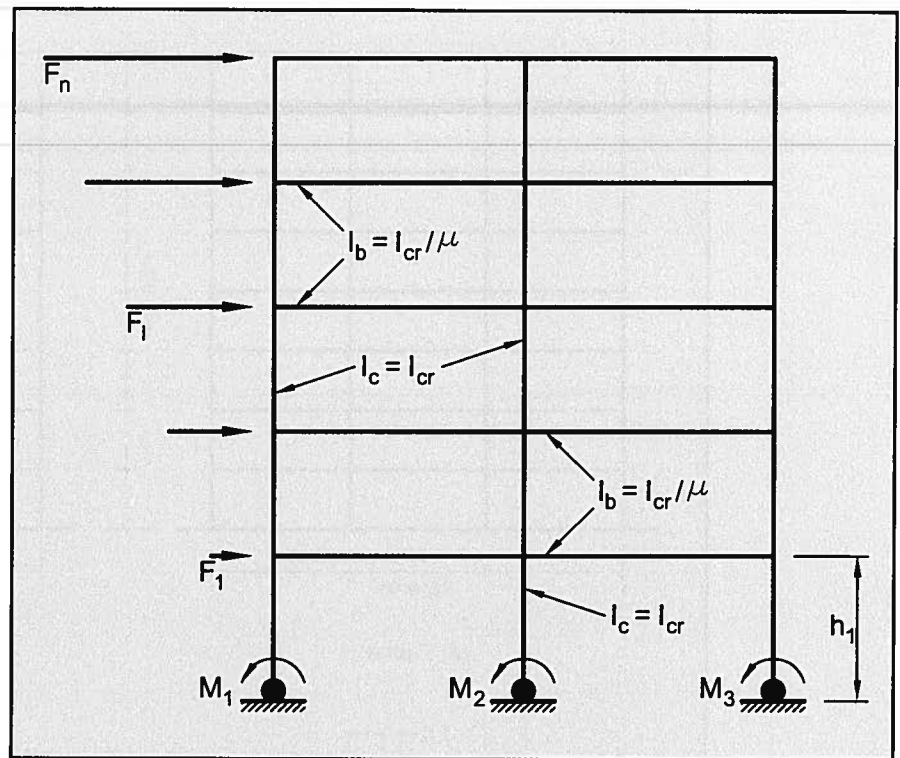


Fig. 6. Analysis of frame building.

tion at maximum displacement response, the structural analysis under the design forces defined by Eq. (19) should use member stiffnesses appropriate to member condition at maximum response. Thus, in a frame building designed for beam hinging, the beam members will be subjected to inelastic actions, and the effective stiffness should be reduced to reflect this.

Referring to the beam moment-rotation response of Fig. 5, the appropriate beam stiffness will be:

$$EI_{eff} = EI_{cr}[1 + r(\mu_b - 1)]/\mu_b \qquad (20)$$

where

$\mu_b$ = expected beam rotation ductility demand

$EI_{cr}$ = cracked section stiffness at effective yield

$r$ = ratio of post-yield to preyield stiffness

Analyses[13] have shown that member forces are not particularly sensitive to the level of stiffness assumed, and thus it is acceptable to assume $EI_{eff} = EI_{cr}/\mu_s$, where $\mu_s$ is the frame design ductility. Since the columns will be designed to remain in the elastic (cracked) range of response, it is appropriate to use the cracked-section

stiffness for these members. An exception occurs at the base of the columns, where plastic hinges can be expected to form.

It has been found[7] that the most effective way to model this is to model the base of the columns as hinges, and apply a base-resisting moment, $M_b$, to the hinge, while representing the column by the cracked-section stiffness. This is represented in Fig. 6, where different moments are applied at the bases of the three columns, in recognition of the influence of the different axial forces on the column strengths.

The values of the moment applied at the column base are to some extent a design choice, since analysis of the structure under the lateral force vector together with the chosen column base moments will ensure a statically admissible equilibrium solution for design moments at all parts of the frame. If the columns are precast, the design base moments will reflect the capacity of the chosen connection detail, with due consideration of the axial force from gravity and seismic loading.

Distribution of design forces between parallel walls should be in proportion to $l_w^2$ where $l_w$ is the wall length. This essentially results in
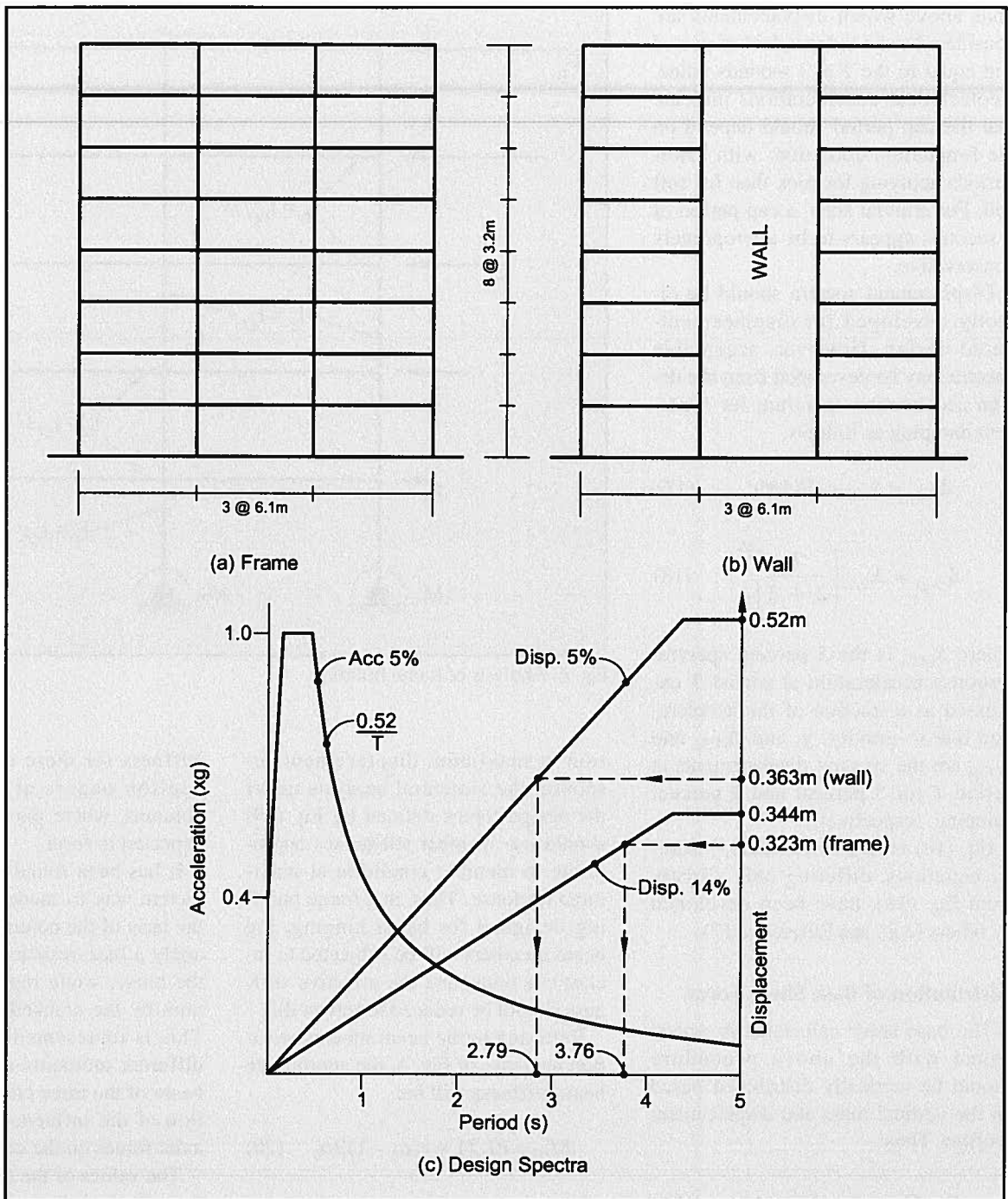
Fig. 7. Direct Displacement-Based Design examples of frames and walls.

Figure labels: (a) Frame; (b) Wall; (c) Design Spectra; 8 @ 3.2m; WALL; 3 @ 6.1m; 3 @ 6.1m; Acceleration (xg); Displacement; Period (s); 1.0; 0.4; Acc 5%; $\frac{0.52}{T}$; Disp. 5%; 0.52m; 0.363m (wall); 0.344m; 0.323m (frame); Disp. 14%; 2.79; 3.76

equal reinforcement ratios, or equal prestress connecting the walls to the base, regardless of the wall length. This is a logical design choice. Note, however, that this differs from force-based design, where the design forces would be distributed in proportion to wall elastic stiffness, and hence to $l_{w}^3$, resulting in the stiffer walls having higher reinforcement ratios than more slender walls.

This unnecessarily underutilizes the potential strength of the more slender walls, and reduces the displacement capacity of the longer walls. More complete details on this topic are provided in Reference 14.

Verification of the DDBD procedure has been provided by extensive inelastic time-history analyses of both frame[13] and wall[14] buildings. In addition, the PRESSS five-story test building, designed by DDBD principles, achieved response displacements within 10 percent of the design values when subjected to an accelerogram representing the design seismic intensity.[4] Additional studies aimed at refining the procedure, and particularly to investigate the significance of higher mode effects, are currently under way.

## DESIGN EXAMPLE

In order to illustrate the simplicity of the direct displacement-based design approach, two different precast options for providing the seismic re-

Table 1. Calculations for DBD design of building in Fig. 7.

| Column 1 | Column 2 | Column 3 | Column 4 | Column 5 | Column 6 | Column 7 | Column 8 |
|---|---|---|---|---|---|---|---|
| Story | Height (m) | FRAME $\Delta$ (m) | DATA $\Delta^2$ | Force (kN) | WALL $\Delta$ (m) | DATA $\Delta^2$ | Force (kN) |
| 1 | 3.2 | 0.063 | 0.0040 | 35.9 | 0.064 | 0.0041 | 66.3 |
| 2 | 6.4 | 0.124 | 0.0154 | 70.6 | 0.128 | 0.0164 | 132.5 |
| 3 | 9.6 | 0.183 | 0.0335 | 104.2 | 0.192 | 0.0369 | 198.8 |
| 4 | 12.8 | 0.240 | 0.0576 | 136.7 | 0.256 | 0.0655 | 265.0 |
| 5 | 16.0 | 0.295 | 0.0870 | 168.0 | 0.320 | 0.1024 | 331.3 |
| 6 | 19.2 | 0.348 | 0.1211 | 198.2 | 0.384 | 0.1475 | 397.5 |
| 7 | 22.4 | 0.399 | 0.1592 | 227.2 | 0.448 | 0.2007 | 463.8 |
| 8 | 25.6 | 0.448 | 0.2007 | 255.1 | 0.512 | 0.2621 | 530.0 |
| SUM = | | 2.100 | 0.6785 | 1196.0 | 2.304 | 0.8364 | 2385.0 |

Note: 1 m = 3.28 ft; 1 kN = 0.225 kip.

sistance of the eight-story structure in Fig. 7 are considered. In Fig. 7a, the bracing system is a hybrid frame, with 50 percent of the beam flexural strength being provided by unbonded prestressing, and 50 percent being provided by bonded reinforcement. The bay lengths are 6.1 m (20 ft), and the beam depth is 762 mm (30 in.).

The second bracing system (see Fig. 7b) for the same building uses unbonded prestressed walls, without additional damping provided by bonded mild reinforcing steel or other means. Thus for this system, the damping, assessed as 5 percent in accordance with Eq. (16c), will be considerably less than for the frame.

The building plan is square [18.3 x 18.3 m (60 x 60 ft)], and story height is 3.2 m (10.5 ft) in both cases. Floor weight is assessed to be 2000 kN (450 kips) per floor, including at the roof level.

The site seismicity is based on IBC[5] requirements for a Site Class C (very dense soil or soft rock), with maximum considered short period spectral response of $S_s = 1.5g$ and maximum considered 1 second spectral response of $S_1 = 0.6g$. The corresponding design acceleration spectrum, shown in Fig. 7c, corresponds closely to the old UBC Zone 4 spectrum.

Also shown in Fig. 7c is the design displacement spectrum for 5 percent damping, found from the acceleration spectrum, using Eq. (17), and conservatively assuming a period cut-off at 4 seconds. Thus, at a response period of 4 seconds, the spectral acceleration is $S_4 = 0.52/4 = 0.13$, and, hence, the corresponding spectral displacement for 5 percent damping is:

$$\Delta_{(4,5)} = 0.13 \times 9.8 \times 4^2/(4\pi^2)$$
$$= 0.52 \text{ m (20.5 in.)}$$

### Frame Required Strength (see Fig. 7a)

**Design Displacement** — The frames bracing the eight-story building for seismic loads will be designed for a maximum drift of $\theta_d = 0.02$ (the maximum permitted by IBC). Substituting $n = 8$ into Eq. (10b) gives the story design displacements at maximum response as:

$$\Delta_i = 0.02h_i\left(1 - 0.125\frac{h_i}{h_n}\right)$$

The story design displacements from this equation are listed in Column 3 of Table 1. The structure design displacement is found from Eq. (5), which, since the floor masses are all equal, simplifies to:

$$\Delta_d = \sum_{i=1}^{n} \Delta_i^2 \bigg/ \sum_{i=1}^{n} \Delta_i$$

Table 1 lists the squared displacements in Column 4, and hence the design displacement is:

$$\Delta_d = 0.6785/2.1$$
$$= 0.323 \text{ m (12.7 in.)}$$

**Yield displacement** — From Eq. (9), the yield drift is:

$$\theta_y = 0.0004 \times 6.1/0.762$$
$$= 0.0032$$

**Displacement Ductility** — In this design, the displacement profile is al-

most linear, and the design displacement ductility can be approximated by:

$$\mu_d = 0.02/0.0032$$
$$= 6.25$$

**Design System Damping** — For a reinforced concrete frame, Eq. (16a) gives the system damping as:

$$\xi = 5 + 30(1 - 6.25^{-0.5})$$
$$= 23.0 \text{ percent}$$

Since 50 percent of the hybrid frame strength is provided by unbonded prestressing steel, the system damping has to be interpolated between Eqs. (16a) and (16c), to give, in this case:

$$\xi = 0.5 \times 23.0 + 0.5 \times 5.0$$
$$= 14.0 \text{ percent}$$

**Effective Mass** — From Eq. (14), the effective mass is:

$$m_e = m_i \sum_{i=1}^{n} \Delta_i \bigg/ \Delta_d$$
$$= (2000/g) \times (2.1/0.323)$$
$$= 13000/g \text{ tonnes}$$

That is, the effective weight is 13000 kN (2925 kips). This corresponds to 81.3 percent of the total building weight.

**Effective Period** — The displacement spectrum for 14 percent damping can be found from Eq. (18). Thus, at a period of 4.0 seconds:

$$\Delta_{(4,14)} = 0.52\left[\frac{7}{2+14}\right]^{1/2}$$
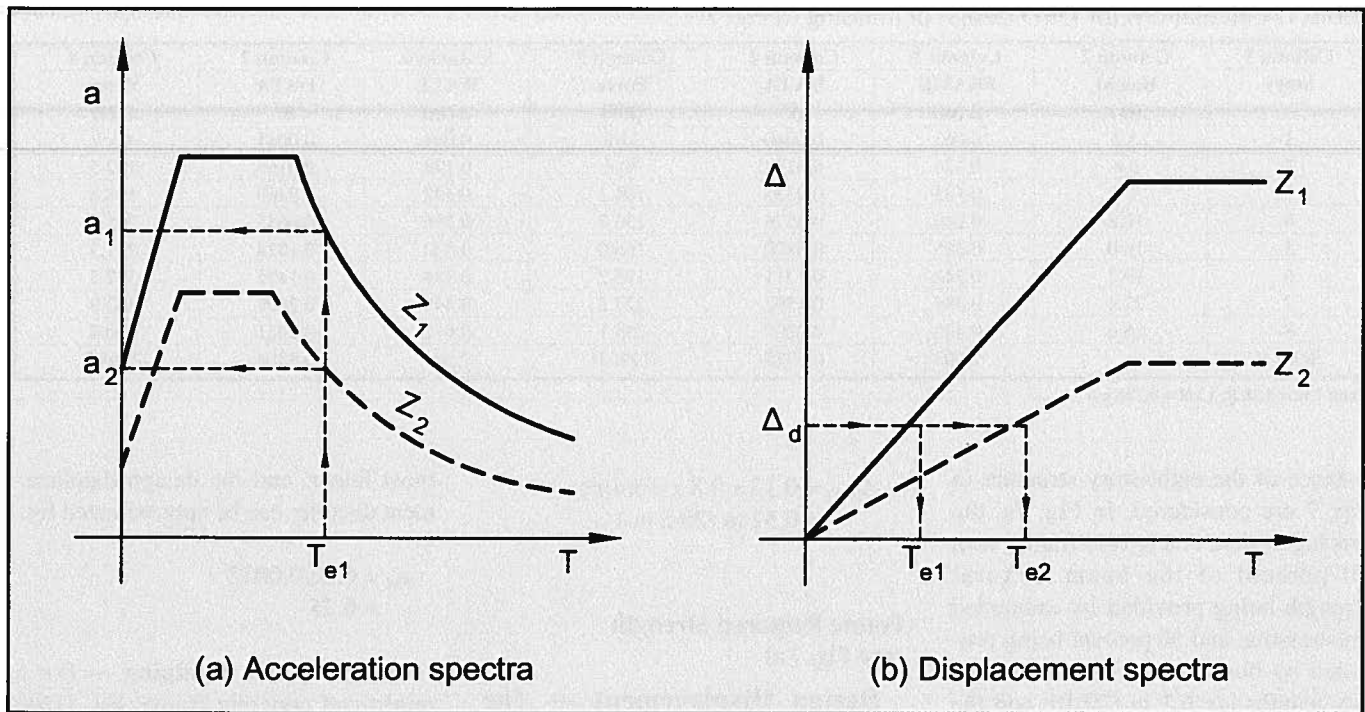$$= 0.344 \text{ m (13.54 in.)}$$

Fig. 8. Influence of zone seismic intensity on design seismic forces.

The displacement spectrum for 14 percent damping is also shown in Fig. 7c. As with the 5 percent damping spectrum, it is linearly proportional to a period above $T = 0.523$ second. Thus, the period corresponding to the design displacement of 0.323 m can be found by proportion as:

$$T_e = 4.0 \times (0.323/0.344)$$
$$= 3.76 \text{ seconds}$$

The procedure is also shown graphically in Fig. 7c by the dashed lines.

**Effective Stiffness** — From Eq. (3), the effective secant stiffness at maximum displacement response is:

$$K_e = 4\pi^2(13000/g)/3.76^2$$
$$= 3704 \text{ kN/m}$$

where the acceleration of gravity was taken as $g = 9.8$ m/s².

**Design Base Shear Force** — Finally, from Eq. (4), the design base shear force at maximum displacement response is:

$$V_B = 3704 \times 0.323$$
$$= 1196 \text{ kN (269 kips)} = 7.5 \text{ per-}$$
cent of building weight

This base shear is distributed between the floors in accordance with Eq. (19), and the results are listed in Column 5 of Table 1. The structure can now be analyzed under these forces to determine the required design moments at maximum displacement response, using the procedures outlined above.

Note that the base shear is the total required for the building, and would be divided between the number of frames participating in seismic resistance. In this case, a peripheral seismic frame system is envisaged, with internal gravity frames. Hence, the required base shear would be 598 kN (134 kips) per frame.

Note that in this case the design effective displacement, and the yield displacement were known before the design started. As a consequence, the damping of 14 percent calculated above is the final value, independent of strength, and no revision to the design, as indicated in Fig. 2, is needed.

In this case, a revision would only have been needed if the initial beam size was altered after the design base shear was determined. If the beam size had been altered, the yield drift, and hence the ductility and damping would have changed, requiring a second

cycle to converge the design process.

**Wall Required Strength (see Fig. 7b)**

**Design Displacement** — As with the frame, the wall is designed for a maximum drift of 0.02. In accordance with Eq. (13b), the design displacement profile is linear, and the design floor level displacements are given in Column 6 of Table 1. The squared displacements are listed in Column 7 of Table 1. Hence, the design displacement is:

$$\Delta_d = 0.8364/2.304$$
$$= 0.363 \text{ m (14.3 in.)}$$

**Yield Displacement** — (Not needed)

**Design System Damping** — 5 percent, as above.

**Effective Mass** — From Eq. (14):

$$m_e = (2000/g) \times (2.304/0.363)$$
$$= 12694/g \text{ tonnes (79.3 percent of total weight)}$$

**Effective Period** — Using the 5 percent displacement spectrum of Fig. 7c,

by linear proportion the effective period is:

$$T_e = 4.0 \times (0.363/0.520)$$
$$= 2.79 \text{ seconds}$$

This is also shown graphically in Fig. 7c.

**Effective Stiffness** — From Eq. (3):

$$K_e = 4\pi^2(12694/9.8)/2.79^2$$
$$= 6569 \text{ kN/m}$$

**Design Base Shear Force** — From Eq. (4):

$$V_B = 6569 \times 0.363$$
$$= 2385 \text{ kN (536 kips)} = 15 \text{ percent of building weight}$$

The floor forces corresponding to this base shear and Eq. (19) are listed as Column 8 of Table 1.

Note that the base shear force for the wall is twice that for the frame. This is because there is no additional (hysteretic) damping for the wall solution, and hence, higher strength is required to limit the displacement to the design values.

If the strength of the wall had been provided by a combination of unbonded prestressing and some energy dissipation system, as was the case for the PRESSS five-story building, the design base shear would have been similar to that of the frame solution. In fact, the solution for the wall design of the PRESSS test building used parallel vertical wall elements connected with rolling plate energy dissipators.

These dissipated more energy than implied by interpolation between Eqs. (16a) and (16c), resulting in a system damping of close to 20 percent. Using this value, the design base shear strength for the wall direction could be reduced below that required for the frame.

## CONCLUDING REMARKS

Direct displacement-based seismic design is a simple procedure for determining the required base shear strength, and hence the critical design bending moments of potential plastic hinges, to ensure that a precast (or conventional structural system) structure responds at the design drift limit. The special characteristics of precast concrete systems, with high ductility and drift capacity, but in some cases reduced damping capacity, can be directly incorporated into the design procedure, which is no more complex than the Equivalent Lateral Force procedure currently specified in American codes.

Use of direct displacement-based design will result in more consistent designs than force-based design criteria, and will generally result in reduced design forces, particularly for regions of moderate seismic intensity, such as the Central and Eastern United States. This is because examination[7] of the fundamental basis of displacement-based design shows that the required strength is proportional to the square of seismic intensity, whereas current force-based design specifies strength directly proportional to zone intensity.

This apparent anomaly can be understood with reference to Fig. 8, which compares acceleration and displacement spectra for two levels of seismic intensity, $Z_1$ and $Z_2$. It is assumed that the spectral shapes for the two levels of intensity are the same. For force-based design, assuming that buildings designed for the two levels of intensity have the same member sizes, the elastic periods will be the same, as will the force-reduction factors, and hence the base shears for similar buildings in the two zones will be directly proportional to the zone intensity. Thus:

$$V_{b2} = V_{b1}(Z_2/Z_1) \tag{21}$$

With DDBD, the design displacements for two similar buildings built in Zones 1 and 2 will be the same (see Fig. 8b), and hence the effective periods $T_1$ and $T_2$ at peak displacement response will be related by:

$$T_2 = T_1(Z_1/Z_2) \tag{22}$$

But from Eqs. (3) and (4), it is seen that the base shear force is inversely proportional to the square of the effective period, and hence:

$$V_{b2} = V_{b1}(Z_2/Z_1)^2 \tag{23}$$

The difference between the results of Eqs. (21) and (23) represents a major outcome of the difference in approach between force-based and displacement-based design.

It is emphasized that, as with force-based design, an integral part of DDBD is the use of capacity design principles[8] to ensure that unintended plastic hinges cannot form, and that energy is dissipated by ductile flexural action, rather than by non-ductile inelastic shear action.

# REFERENCES

1. Priestley, M. J. N., "The PRESSS Program – Current Status and Proposed Plans for Phase III," PCI JOURNAL, V. 41, No. 2, March-April 1996, pp. 22-40.

2. ACI Innovation Task Group 1 and Collaborators, "Acceptance Criteria for Moment Frames Based on Structural Testing (ACI ITG/T1.1-01)," American Concrete Institute, Farmington Hills, MI, 2001.

3. ACI Innovation Task Group 1 and Collaborators, "Special Hybrid Moment Frames Composed of Discretely Jointed Precast and Post-Tensioned Concrete Members (ACI T1.2-XX) and Commentary (T1.2R-XX)," *ACI Structural Journal*, V. 98, No. 5, September-October 2001, pp. 771-784.

4. Priestley, M. J. N., Sritharan, S., Conley, J. R., and Pampanin, S., "Preliminary Results and Conclusions From the PRESSS Five-Story Precast Concrete Test Building," PCI JOURNAL, V. 44, No. 6, November-December 1999, pp. 42-67.

5. ICC, *IBC 2000 International Building Code*, International Code Council, Falls Church, VA, 2000.

6. Fajfar, P., and Krawinkler, H. (Editors), "Seismic Design Methodologies for the Next Generation of Building Codes," Proceedings of an International Conference at Bled, Slovenia, A. A. Balkema, Rotterdam/Brookfield, 1997, 411 pp.

7. Priestley, M. J. N., "Performance Based Seismic Design," Keynote Address, 12th World Conference on Earthquake Engineering, Auckland, New Zealand, January 2000.

8. Paulay, T., and Priestley, M. J. N., *Seismic Design of Reinforced Concrete and Masonry Buildings*, John Wiley & Sons, New York, NY, 1992.

9. Shibata, A., and Sozen, M., "Substitute Structure Method for Seismic Design in Reinforced Concrete," *Journal of Structural Engineering*, American Society of Civil Engineers, V. 102, No. 12, pp. 3548-3566.

10. Sozen, M. A., "Review of Earthquake Response of R/C Buildings with a View to Drift Control," *State-of-the-Art in Earthquake Engineering*, O. Ergunay and M. Erdik (Editors), Ankara, Turkey, 1981, pp. 383-418.

11. Priestley, M. J. N., and Kowalsky, M. J., "Aspects of Drift and Ductility Capacity of Cantilever Structural Walls," *Bulletin*, NZ Society for Earthquake Engineering, V. 31, No. 2, June 1998.

12. Priestley, M. J. N., "Brief Comments on Elastic Flexibility of Reinforced Concrete Frames, and Significance to Seismic Design," *Bulletin*, NZ Society for Earthquake Engineering, V. 31, No. 4, December 1998.

13. Loeding, S., Kowalsky, M. J., and Priestley, M. J. N., "Direct Displacement-Based Design of Reinforced Concrete Frame Buildings," Report SSRP 98/08, University of California, San Diego, CA, 1998.

14. Priestley, M. J. N., and Kowalsky, M. J., "Direct Displacement-Based Design of Concrete Buildings," *Bulletin*, NZ Society for Earthquake Engineering, V. 33, No. 4, December 2000.

15. Otani, S., "Hysteresis Models for Reinforced Concrete for Earthquake Response Analysis," *Journal*, Faculty of Engineering, University of Tokyo, Tokyo, Japan, V. XXXVI, No. 2, 1981, pp. 125-159.

16. EC8, *Eurocode (2000), Design Provisions for Earthquake Resistance of Structures*, Lausanne, Switzerland.

17. SEAOC Seismology Committee, *SEAOC Recommended Lateral Force Requirements and Commentary*, 7th Edition, Structural Engineers Association of California, Sacramento, CA, 1999.

# APPENDIX A — NOTATION

$C_1$ = coefficient dependent on structural system

$C_T$ = basic seismic coefficient dependent on seismic intensity, soil condition and period $T$

$D$ = diameter of circular column

$d_{EP}$ = residual displacement for elasto-plastic system

$d_{RC}$ = residual displacement for reinforced concrete system

$d_J$ = residual displacement for jointed system

$E$ = Young's modulus of elasticity

$F_i$ = inertia force at $i$

$g$ = acceleration of gravity

$h_b$ = depth of beam

$h_i$ = height to $i$th story

$h_n$ = building height

$h_c$ = depth of rectangular column

$I$ = importance factor reflecting different levels of acceptable risk for different building functions

$I_{cr}$ = moment of inertia of cracked section at effective yield

$I_{eff}$ = moment of inertia adjusted for ductility

$K_e$ = effective stiffness at maximum displacement

$l_w$ = depth of wall

$l_b$ = bay length

$l_p$ = plastic hinge length

$m_e$ = effective mass

$m_i$ = story mass

$n$ = number of stories

$r$ = ratio of post-yield to pre-yield stiffness

$R_\mu$ = force reduction factor, dependent on ductility capacity ($\mu$) of structural form and material

$S_4$ = spectral acceleration at a response period of 4 seconds

$S_{(T,5)}$ = 5 percent spectral response acceleration at period $T$

$T$ = period

$T_e$ = effective period at maximum displacement

$T_1$ = effective period at peak displacement response for building in specified seismicity Zone 1

$T_2$ = effective period at peak displacement response for building in specified seismicity Zone 2

$V_B$ = required base shear strength

$V_{b1}$ = required base shear strength for force based design in specified seismicity Zone 1

$V_{b2}$ = required base shear strength in specified seismicity Zone 1

$Z_1$ = level of seismicity, Zone 1

$Z_2$ = level of seismicity, Zone 2

$\Delta_d$ = design displacement of SDOF structure

$\Delta_i$ = design displacement at story $i$

$\Delta_y$ = yield displacement

$\Delta_{(T,5)}$ = spectral displacement at period $T$ for 5 percent damping

$\Delta_{(T,\xi)}$ = spectral displacement at period $T$ for $\xi$ percent damping

$\Delta_{(4,5)}$ = spectral displacement with a period of 4 seconds for 5 percent damping

$\Delta_{(4,14)}$ = spectral displacement with a period of 4 seconds for 14 percent damping

$\varepsilon_y$ = yield strain of flexural reinforcement

$\phi_m$ = maximum curvature

$\phi_y$ = yield curvature

$\mu$ = ductility capacity

$\mu_b$ = expected beam rotation ductility demand

$\mu_s$ = frame design ductility

$\pi$ = 3.14159

$\theta_c$ = code limit drift

$\theta_d$ = design drift

$\theta_p$ = plastic component drift

$\theta_y$ = elastic component drift

$\xi$ = percentage of critical damping